

# THE POLARIZATION EFFECTS OF RADIATION FROM MAGNETIZED ENVELOPES AND EXTENDED ACCRETION STRUCTURES

Gnedin Yu.N.<sup>1</sup>, Silant'ev N.A.<sup>1,2</sup>  
Piotrovich M.Yu.<sup>1</sup>, Pogodin M.A.<sup>1</sup>

November 19, 2018

(1) Central Astronomical Observatory at Pulkovo, Saint-Petersburg, Russia.

(2) Instituto National de Astrofisica, Optica y Electronica, Apartado Postal 51 y 216, C.P. 72000, Pue. Mexico.

## Abstract

The results of numerical calculations of linear polarization from magnetized spherical optically thick and optically thin envelopes are presented. We give the methods how to distinguish magnetized optically thin envelopes from optically thick ones using observed spectral distributions of the polarization degree and the positional angle. The results of numerical calculations are used for analysis of polarimetric observations of OB and WR stars, X-ray binaries with black hole candidates (Cyg X-1, SS 433) and supernovae. The developed method allows to estimate magnetic field strength for the objects mentioned above.

## 1 INTRODUCTION

The existence of magnetic fields in hot stellar atmospheres and envelopes as well as in accretion envelopes of quasars and AGNs gives rise to the Faraday rotation of the polarization plane of the radiation from these objects. The angle of the Faraday rotation  $\psi$  may be written in the form [1]:

$$\psi(\mathbf{n}, \mathbf{B}) = \frac{1}{2}\delta\tau_T \cos\Theta, \quad (1)$$

$$\delta = \frac{3}{4\pi} \cdot \frac{\lambda}{r_e} \cdot \frac{\omega_B}{\omega} \cong 0.8\lambda^2(\mu\text{m})B(G). \quad (2)$$

where  $\mathbf{n}$  is the direction of wave propagation,  $\Theta$  is the angle between  $\mathbf{n}$  and magnetic field  $\mathbf{B}$ ,  $\tau_T$  is the Thomson optical length ( $\tau_T = N_e\sigma_T l$ ),  $N_e$  is the electron number density,  $l$  is the geometric path,  $\sigma_T = 8\pi r_e^2/3$  is Thomson's cross-section,  $r_e = e^2/mc^2 \approx 2.82 \times 10^{-13}$  cm is the classic radius of electron,  $\omega_B = |e|B/mc$  is the cyclotron frequency,  $\omega = 2\pi c/\lambda = kc$  is the frequency of radiation ( $\omega_B/\omega \approx 0.93 \times 10^{-8}\lambda(\mu\text{m})B(G)$ ).

At large distances from a star or a quasar magnetic field is approximately dipolar because other multipoles fall off with distance more rapidly than the dipole component. Because of small value of Thomson's cross-section  $\sigma_T$  the optically thick envelopes seem to be seldom the case. The expanding matter just after the supernova explosion, when the concentration of particles is yet large enough, is possibly a case of such optically thick envelope. Another example may be the accretion structures near quasars and AGNs.

Magnetospheres around the black holes of different masses have to play a very important role in formation of various structures of outflowing matter (winds, expanding coronae, jets, etc.). Possible existence of such magnetospheres was confirmed recently both by spectroscopic (Robertson and Leiter [2]) and by polarimetric (Gnedin et al. [3]) observations of X-ray binary systems with black holes.

Now the Blandford and Znajek mechanism is commonly accepted which provides the energy extraction from a rotating black hole by means of magnetic field [4].

Later this idea was developed in papers [5-7]. In these papers the model was considered where the toroidal electric current at the inner boundary of the accretion disk generates the dipole magnetic field connecting together the black hole horizon and the region of the accreting disk beyond its inner boundary.

The plasma outflow from the magnetosphere and the inner part of accretion disk gives rise to an envelope. The radiation scattered in the envelope acquires the linear polarization. The region of the formation of broad emission lines observed in AGNs is a case of such envelope.

In the absence of magnetic field the scattered radiation has to be non-polarized provided the scattering matter in the spherically shape envelope is symmetric relative to the line of sight. If the magnetic field of the object is not symmetric relative to this line, the outgoing radiation (singly or multiply scattered) has to undergo influence of the Faraday's rotation effect and becomes to be polarized. The integral polarization of radiation is equal to zero if the dipole magnetic momentum  $\mathbf{M}$  is coaxial with the line of sight or in the case of  $\mathbf{B} = 0$ .

## 2 OPTICALLY THIN ENVELOPE

The integral polarization scattered in an envelope is simplest to calculate if the envelope is optically thin. In this case we can take into account only single scattered radiation and the Faraday rotation during the followed propagation to an observer. This was made for various types of envelopes in papers [8-10], where, however, was accepted that a star is a point-like source of non-polarized radiation. This assumption gives rise to some overestimation of the polarization degree (more detailed, see below). Maximal disturbance of axial symmetry of the Faraday's rotation picture occurs when magnetic dipole  $\mathbf{M}$  is perpendicular to line of sight  $\mathbf{n}$  ( $\vartheta_m = 90^\circ$ ). In this case the integral polarization from the whole envelope acquires its maximum value and the polarization plane coincides with the plane ( $\mathbf{nM}$ ).

The polarization Stokes parameters  $F_Q$  and  $F_U$ , according to [1, 8, 9], are described by the following expressions:

$$F_Q(\mathbf{n}) = -\frac{L}{4\pi R^2} \cdot \frac{3}{16\pi} \sigma_T \int dV \frac{N_e(\mathbf{r})}{r^2} \sqrt{1 - \frac{R_s^2}{r^2}} \sin^2 \vartheta \cos 2(\varphi + \psi), \quad (3)$$

$$F_U(\mathbf{n}) = -\frac{L}{4\pi R^2} \cdot \frac{3}{16\pi} \sigma_T \int dV \frac{N_e(\mathbf{r})}{r^2} \sqrt{1 - \frac{R_s^2}{r^2}} \sin^2 \vartheta \sin 2(\varphi + \psi), \quad (4)$$

where  $L(\text{erg s}^{-1} \text{Hz}^{-1})$  is the luminosity of the central star,  $R$  is the distance from the star to the telescope, the angles  $\vartheta$  and  $\varphi$  determine the direction of the radius vector  $\mathbf{r}(r, \vartheta, \varphi)$ ;  $R_s$  is the radius of the star. Integration yields over the visible part of the envelope volume. In (3) and (4) we accepted that X-axis lies in the plane ( $\mathbf{nM}$ ).

Near the stellar surface the polarization of the scattered radiation is small because of the non-polarized star's radiation is falling to the volume element  $dV$  practically isotropic from the solid angle  $\approx 2\pi$ . In the book [1](chapter 4) the formulae are given which describes this effect quantitatively. There was considered the commonly used model when the intensity  $I(\mu)$  of outgoing radiation is approximated by the formula  $I(\mu) = A + C\mu$ . Remember that  $\mu$  is the cosine of the angle between the normal to the atmosphere's surface and the direction of the escaping photons. In this paper we consider only the isotropic case ( $C = 0$ , Lambert's law of radiation) when the effect of depolarization of scattered radiation near the stars's surface is maximal (most profound). This gives rise to the factor  $\sqrt{1 - R_s^2/r^2}$  in formulae (3) and (4) as compared with the analogous formulae in [8-10] where a star was considered as point-like source of non-polarized radiation. The non point-like character of the radiation source was taken into account first in [11].

We restrict ourselves by two types of the electron number density  $N_e(\mathbf{r})$  in an envelope:  $N_e(r) = N_0 = \text{const}$  and  $N_e(\mathbf{r}) = N_0(R_s^2/r^2)$ . The explicit formulae for Faraday's rotation angle  $\psi$  have the form [8]:

For the envelope with  $N_e(r) = \text{const}$

$$\psi = \frac{\delta_s \tau_{env}}{2(\eta - 1)\rho^2} \{ \cos \vartheta_m [\cos \vartheta - \frac{\rho^2}{\eta^2} \sqrt{1 - \frac{\rho^2}{\eta^2} \sin^2 \vartheta}] + \sin \vartheta_m \cos \varphi \sin \vartheta (1 - \frac{\rho^3}{\eta^3}) \}. \quad (5)$$

Here,  $\eta = R_0/R_s$  is the ratio of the envelope radius  $R_0$  to the radius of a star  $R_s$ ;  $\rho = r/R_s$ ,  $\delta_s = 0.8\lambda^2 M/R_s^3$  is the Faraday's depolarization parameter (2) at the magnetic equator of the star,  $M$  is

Table 1: The coefficients  $K_Q$ ,  $K_U$  and the maximal polarization degree for the various values of the parameter  $\eta$  (the model of a non-point like source of radiation).

$\eta$	1.02	1.05	1.1	1.2	1.5	2	3	4	5
100 $K_Q$	0.747	1.116	1.362	1.376	0.830	0.325	0.078	0.028	0.013
100 $K_U$	-2.644	-2.944	-2.593	-1.638	-0.375	-0.048	-0.002	-0.000	$-3 \cdot 10^{-5}$
$\frac{P_l \max}{\tau_{env}} (\%)$	0.974	1.650	2.457	3.566	5.252	6.075	6.081	5.964	5.841
$\sqrt{\delta_s \tau_{env}}$	1.40	1.45	1.50	1.65	2.10	2.80	5.05	7.60	10.30

Table 2: The same values for the model of a point like star.

$\eta$	1.02	1.05	1.1	1.2	1.5	2	3	4	5
100 $K_Q$	8.018	7.593	6.631	4.892	2.065	0.662	0.139	0.048	0.022
100 $K_U$	-28.32	-19.67	-12.27	-5.592	-0.869	-0.086	-0.003	-0.000	-0.000
$\frac{P_l \max}{\tau_{env}} (\%)$	8.136	8.728	9.310	9.830	10.03	9.241	7.403	6.609	6.234
$\sqrt{\delta_s \tau_{env}}$	1.30	1.35	1.40	1.55	1.90	2.55	3.65	6.30	10.00

magnetic dipole moment of the star,  $\tau_{env} = N_0 \sigma_T (R_0 - R_s)$  is Thomson's optical depth of the envelope,  $\vartheta_m$  is the angle between  $\mathbf{M}$  and line of sight  $\mathbf{n}$ .

For the envelope with  $N_e = N_0 (R_s^2 / r^2)$ :

$$\psi = \frac{\delta_s \tau_{env}}{2\rho^4 \sin^4 \vartheta} \{ \cos \vartheta_m [-(1 - \cos \vartheta) + \frac{4}{3}(1 - \cos^3 \vartheta) - \frac{3}{5}(1 - \cos^5 \vartheta)] + \frac{3}{5} \sin \vartheta_m \cos \varphi \sin^5 \vartheta \}. \quad (6)$$

Here,  $\tau_{env} = N_0 \sigma_T R_s$  is the optical depth of the envelope. Remind that for single scattered radiation ( $\tau_{env} \ll 1$ ) we neglect the terms  $\sim \tau^2$  and higher. On this approximation when calculating the polarization degree  $p_l = \sqrt{F_Q^2 + F_U^2} / F_l$  one can take for the flux  $F_l$  the value  $L / 4\pi R^2$ .

It follows from (3) and (4) that  $F_Q$  and  $F_U$  have the form:

$$F_{Q,U} = F_l \tau_{env} f_{Q,U}(\delta_s \tau_{env}, \vartheta_m, \eta). \quad (7)$$

For the envelope with  $N_e \sim r^{-2}$  the variable  $\eta$  in (7) is absent.

For weak magnetic fields or large wavelenghtes, when  $\psi \ll 1$ , the  $f_{Q,U}$  functions have the following asymptotic form:

$$f_Q \simeq K_Q (\delta_s \tau_{env})^2 \sin^2 \vartheta_m,$$

$$f_U \simeq K_U (\delta_s \tau_{env})^3 \cos \vartheta_m \sin^2 \vartheta_m. \quad (8)$$

The case  $\psi \ll 1$  corresponds to  $\delta_s \tau_{env} \ll 1$ . It means that  $|f_U| \ll |f_Q|$ , i.e. the wave electric field oscillates near the plane  $(\mathbf{nM})$  and the polarization degree  $p_l \approx \tau_{env} |f_Q|$ . The asymptotic formulae (8) take place up to  $\delta_s \tau_{env} \approx 1$ .

The numerical coefficients  $K_Q$  and  $K_U$  for the case  $N_e \sim r^{-2}$  are equal to 0.0006641 and -0.0000796, correspondingly. For the model of point-like source of radiation these values are considerably larger: 0.0016136 and -0.0001873. In the case  $N_e = \text{const}$  the coefficients  $K_Q$  and  $K_U$  depend on the parameter  $\eta = R_0 / R_s$ . The numerical values of  $K_Q(\eta)$  and  $K_U(\eta)$ , as functions of  $\eta$ , for non point-like star, are presented in Table 1. It should be noted that for  $\eta < 1.15$  ( $K_Q(1.15) = 0.014136$ ,  $K_U(1.15) = -0.02088$ ) the polarization of radiation decreases. This fact reflects the effect of depolarization of scattered radiation near the star surface, mentioned above. On the contrary the values of  $K_Q(\eta)$  and  $K_U(\eta)$  for the point-like star model (see, Table 2) increase monotonously with  $\eta \rightarrow 1$ . The negative sign of  $K_U$  denotes that the positional angle  $\chi$  ( $\tan 2\chi = f_U / f_Q$ ) is also negative, i.e. corresponds to left-hand rotation of the wave electric fields from the plane  $(\mathbf{nM})$ , for the line of sight  $\mathbf{n}$ .

The values  $p_l/\tau_{env} = \sqrt{(f_Q^2 + f_U^2)}$  (in %) and the positional angle  $\chi$  (in degrees), as the functions of  $\sqrt{\delta_S \tau_{env}}$ , are presented in Fig.1. Remember that the X-axis lies in the plane  $(\mathbf{nM})$ . The upper panels correspond to  $N_e(r) = N_0(R_S/r)^2$  and the lower ones correspond to envelope with  $N_e = const$  and  $\eta = 5$ . All curves represent the model of non-point-like star. For the polarization degree to be obtained the right-hand curves must be multiplied by the optical depth  $\tau_{env} < 1$ .

For optically thin envelopes the maximum polarization  $p_{lmax}$  (at  $\vartheta_m = 90^\circ$ ) can acquire rather considerable values  $\sim 6\tau_{env}(\%)$  for the non-point-like star (see Table 1) and  $\sim 10\tau_{env}(\%)$  for point-like model of the radiation source (see Table 2). In these tables we present the values of  $\sqrt{\delta_S \tau_{env}}$  corresponding to  $p_{lmax}$  values.

It is notable that  $p_{lmax}$  is almost the same for various geometric depths of the envelopes ( $\eta \simeq 1.5 \div 5$  for non-point-like stars) and ( $\eta \simeq 1.02 \div 3$  for point-like model). Only the corresponding values of  $\sqrt{\delta_S \tau_{env}}$  parameter change its position. Considering the fixed value  $\tau_{env}$  for all envelopes we can interpret the mentioned fact as for every envelope there exists the effective layer with  $\psi \approx 1$  which gives the main contribution to the integral polarization. The interval of  $\sqrt{\delta_S \tau_{env}}$ , corresponding to  $p_{lmax}$ , increases with the increasing of the envelope radius  $R_0$ . For  $\eta = 2$  this interval (the width of the polarization spectrum) corresponds to  $\sqrt{\delta_S \tau_{env}} \approx 2 \div 5$ . For  $\eta = 5$  this width corresponds to  $\sqrt{\delta_S \tau_{env}} \approx 4 \div 20$ .

With increasing magnetic field this effective layer shifts from the stellar surface up to the outer boundary of the envelope. For further increasing of  $\mathbf{B}$  the polarization is determined by the thin boundary layer where  $\psi \leq 1$ . This condition takes place at the optical depth of this layer  $\tau \sim 1/\delta_0 \propto \lambda^{-2}$ , where  $\delta_0 = 0.8\lambda^2 M/R_0^3$  is the parameter (2) at the outer boundary of the envelope. This estimation assumes that the total inner volume does not give a contribution to integral polarization, i.e.  $\delta_s \tau_{env}/\eta^3 \gg 1$ . The intensity of the radiation scattered in this thin layer is proportional to  $\tau$ . It means that the integral polarization is also inversely proportional to  $\delta_0$ , i.e.  $p_l \simeq C(\vartheta_m)\eta^3/\lambda^2$ . The analytical formula for  $\vartheta_m = 90^\circ$  gives:

$$p_l \approx \frac{\pi\eta^3}{16\delta_s} \sqrt{1 - \frac{1}{\eta^2}} \propto \frac{1}{\lambda^2}, \quad \frac{\delta_s \tau_{env}}{\eta^3} \gg 1. \quad (9)$$

Asymptotic dependence  $p_l \propto \lambda^{-2}$  takes place for  $\delta_s \tau_{env}/\eta^3 \approx 50 \div 100$ . The expression (9) was obtained without the exclusion of invisible part of the envelope, i.e. it gives rather overestimated value for  $p_l$ . So, for  $\eta = 2$  the overestimation is equal to 11% at  $\sqrt{\delta_S \tau_{env}} = 1$  and equal to 3% for  $\sqrt{\delta_S \tau_{env}} = 10$ . For more vast envelope with  $\eta = 5$  the corresponding values are 6% and 0.6%. For the model with  $N_e \propto r^{-2}$  these values of overestimation are equal to 15% and 2%, correspondingly. If  $\eta \rightarrow 1$ , the invisible part of the envelope are practically the half of all the envelope volume. Therefore, for this case we need to diminish the value (9) to 2 times.

As it was showed in [1], a star can be considered as a point-like source of non-polarized radiation from the distances  $(1 \div 2)R_s$  from the star surface. Therefore, the asymptotic values of polarization at  $\delta_S \tau_{env} \gg 1$  are the same for both models of point-like and non-point-like sources, if, of course, the geometric depth of an envelope is larger than  $(2 \div 3)R_s$ .

For envelopes with  $N_e \sim r^{-2}$  the peak of polarization (at  $\vartheta_m = 90^\circ$ ) occurs at  $\sqrt{\delta_S \tau_{env}} \approx 4.65$  and equal to  $2.886\tau_{env}(\%)$  for the case of non point-like model. The point-like model for the same value  $\sqrt{\delta_S \tau_{env}} \approx 4.65$  gives  $3.878\tau_{env}(\%)$ . The peak polarization for point-like star model occurs at  $\sqrt{\delta_S \tau_{env}} \approx 3.05$  and is equal to  $4.722\tau_{env}(\%)$ .

Asymptotic behavior of polarization at  $\sqrt{\delta_S \tau_{env}} \gg 1$  and  $N_e \sim r^{-2}$  is determined also by outer layer of the envelope ( $r \geq r_*$ ) where  $\psi(r_*) = 0.5\delta(r_*)\tau(r_*) \leq 1$ . The optical depth of this layer is equal to  $\tau(r_*) = t_{env}R_S/r_*$ , where  $\delta(r_*)$  is the value of parameter (2) at this boundary  $r = r_*$ . Taking into account that  $\delta(r_*) \propto 1/r_*^3$ , we obtain  $r_* \propto \sqrt{\lambda}$ . This means  $p_l \propto 1/\sqrt{\lambda}$ . To calculate the polarization at large values of the parameter  $\sqrt{\delta_S \tau_{env}}$  we can, as in previous case, take the numerical value at  $\sqrt{\delta_S \tau_{env}} = 10$  from the Fig.1 and extrapolate it, using asymptotic dependence on  $\lambda$ . For  $\vartheta_m = 90^\circ$  and  $N_e \sim r^{-2}$  one yields the formula:

$$f_Q \approx \frac{0.086}{(\delta_s \tau_{env})^{1/4}}, \propto \frac{1}{\sqrt{\lambda}}, \quad \delta_s \tau_{env} \gg 1. \quad (10)$$

Thus, for  $N_e \sim r^{-2}$  the polarization degree decreases as  $\sim 1/\sqrt{\lambda}$ . Using qualitative derivation of  $p_l(\lambda)$  at  $\sqrt{\delta_s \tau_{env}} \gg 1$ , given above, one can derive for  $N_e \propto r^{-\nu}$  the following asymptotic  $\lambda$ -dependence  $p_l \propto \lambda^{-2(\nu-1)/(\nu+2)}$ .

The polarization at  $\delta_S \tau_{env} \gg 1$  is determined by the contribution of the envelope's volumes far from the central source. It means that both the polarization degree and the positional angle give an information about number density  $N_e(r)$  and magnetic field  $\mathbf{B}(\mathbf{r})$  just in this part of the envelope. So, polarimetric observations can determine (or to prove some accepted model) the distribution of free electrons in the envelope.

### 3 OPTICALLY THICK ENVELOPE

To calculate the integral polarization of radiation from optically thick envelopes one has to know the intensity  $I$  and the Stokes parameters  $Q$  and  $U$  of the radiation outgoing from an element of the surface of the envelope. We assume that the sources of radiation with the considered wavelength  $\lambda$  are distributed far from the outer surface of the envelope, i.e. the parameters  $I, Q, U$  are the solution of the classic Milne's problem for semiinfinite plane-parallel atmosphere with taking into account the Faraday rotation of the polarization plane. This problem was solved numerically (see, [12, 13]) only for the magnetic field directed along the normal to the atmosphere. For the arbitrary direction of magnetic field the problem is too complicated and is not solved yet. Considering the dipole, i.e. non-homogeneous, magnetic field we are to know the solution of the Milne problem for arbitrary magnetic field direction.

In the paper [14] the simple asymptotic formulae (at  $\delta_0 \geq 1$ ) for  $I, Q, U$  are derived for a number of radiative transfer problems, including the Milne problem. It is important that these analytic formulae are suitable for the arbitrary direction of magnetic field. They give exact solutions for large values of the depolarization parameter  $\delta$  (see (2)). These formulae correspond to the approximation when the intensity of radiation is found from the usual scalar radiation transfer equation with the Rayleigh phase function and the polarization is calculated as a result of single scattering of known radiation flux before the outgoing from the semiinfinite atmosphere. The transformation of this single scattered radiation due to Faraday's rotation effect is also taken into account. These formulae give to some extent overestimated values for the polarization. The comparison with the exact numerical results for magnetic field directed along the normal to the atmosphere shows that for the conservative case ( $q = \sigma_a/(\sigma_a + \sigma_T) = 0$ ) these asymptotic formulae give the correct result with the relative error of 10% at  $\delta_0 = 10$ . For  $\delta_0 = 5$  the error is larger and is equal to  $\approx 20\%$ . For absorbing atmosphere ( $q \neq 0$ ) these asymptotic formulae are less exact than for more important case  $q = 0$ .

The use of these simple asymptotic formulae (see [14]) gives rise to the following expressions for the Stokes parameters of the radiation from an optically thick magnetized spherical envelope:

$$F_I = \frac{a^2}{R^2} F, \quad (11)$$

$$F_Q = -\frac{a^2}{R^2} \cdot \frac{F}{\pi J_1} \cdot \frac{1-g}{1+g} \int_0^1 d\mu \int_0^\pi d\varphi \mu(1-\mu^2) \frac{(1-k\mu) \cos(2\varphi)}{(1-k\mu)^2 + [(1-q)\delta \cos \Theta]^2}, \quad (12)$$

$$F_U = -\frac{a^2}{R^2} \cdot \frac{F}{\pi J_1} \cdot \frac{1-g}{1+g} \int_0^1 d\mu \int_0^\pi d\varphi \mu(1-\mu^2) \frac{(1-q)\delta \cos \Theta \cos(2\varphi)}{(1-k\mu)^2 + [(1-q)\delta \cos \Theta]^2}. \quad (13)$$

Here,  $F$  is the radiation flux from the  $1 \text{ cm}^2$  of the envelope surface,  $a$  is the outer radius of the envelope,  $R$  is the distance to an observer, the numerical factors  $J_1$  and  $g$  depend on  $q$  and are calculated in [14]. The value  $\delta \cos \Theta$  for the dipole magnetic field is equal to

$$\delta \cos \Theta = \delta_0 [(3\mu^2 - 1) \cos \vartheta_m + 3\mu \sqrt{1 - \mu^2} \sin \vartheta_m \cos \varphi], \quad (14)$$

where  $\delta_0 = 0.8\lambda^2 M/a^3$  is the parameter (2) at the magnetic equator of outer surface of the envelope.

Further, we shall consider also two cases of the distorted dipole magnetic field: 1) diamagnetic (perfectly conducting) envelope when the normal component of the magnetic field does not penetrate into medium, and 2) the envelope with the strong plasma radial outflow when the frozen magnetic field acquires the radial form (this is the analogy of Parker's spherically symmetric wind for non-rotating star). The envelope can be considered as diamagnetic one when the ohmic diffusion characteristic time ( $\tau_{ohm} \approx a^2/6D_m$  with ohmic diffusion coefficient  $D_m = c^2/4\pi\sigma$ ) is much lesser than others characteristic times (the time of turbulent mixing, period of cyclotron rotation and so on (see [15])).

For diamagnetic envelope the radial component  $B_r$  of the dipole magnetic field are to be excluded. This gives the expression:

$$\delta \cos \Theta = \delta_0 [-\cos \vartheta_m (1 - \mu^2) + \mu \sqrt{1 - \mu^2} \sin \vartheta_m \cos \varphi]. \quad (15)$$

For the Parker outflow, on the contrary, only  $B_r$  must be taken into account:

$$\delta \cos \Theta = 2 \delta_0 (\mu^2 \cos \vartheta_m + \mu \sqrt{1 - \mu^2} \sin \vartheta_m \cos \varphi). \quad (16)$$

In Figures the cases (14), (15) and (16) are denoted as a), b) and c).

For small values of the depolarization parameter  $\delta_0 \ll 1$  and the most interesting case of conservative atmosphere ( $q = 0$ ) the integrals (12) and (13) can be easily calculated analytically. In this case we have  $F_Q \propto \delta_0^2$  and  $F_U \propto \delta_0^3 \ll F_Q$ . It gives  $p_l = \sqrt{F_Q^2 + F_U^2}/F_I$  and  $\tan 2\chi = F_U/F_Q$ . Finally we obtain

$$p_l \simeq C \delta_0^2 \sin^2 \vartheta_m, \quad (17)$$

$$\chi \simeq D \delta_0 \cos \vartheta_m, \quad (18)$$

where the coefficients  $C$  and  $D$  for the cases (14), (15) and (16) are equal to:  $C = 0.765$ ,  $D = 17.19$  for the dipole (14);  $C = 0.0797$ ,  $D = -51.56$  for the diamagnetic envelope (15);  $C = 0.319$ ,  $D = 68.75$  for the radial outflow (16). It should be noted that X-axis is chosen in the plane "line of sight - magnetic dipole" ( $\mathbf{nM}$ ). The positive  $\chi$  corresponds for an observer to the anticlockwise deviation from this plane ( $\mathbf{nM}$ ). If the magnetic dipole  $\mathbf{M}$  has  $\vartheta = 90^\circ$ , the sign of the positional angle  $\chi$  is opposite.

Eqs. (17) and (18) show that  $p_l \propto \lambda^4$  and  $\chi \propto \lambda^2$ . The comparison with numerical calculations demonstrates that eqs. (17) and (18) are valid up to  $\delta_0 = 0.25$ .

## 4 DISCUSSIONS OF THE RESULTS

Numerical calculations of  $p_l$  and  $\chi$  from (11)-(13) are presented in Fig.2-5 as functions of dimensionless parameter  $\sqrt{\delta_0} \cong 0.89 \lambda(\mu m) \sqrt{B_0(G)}$ , where  $B_0 = M/a^3$  is the magnetic field on the surface of optically thick spherical envelope. Parameter  $\sqrt{\delta_0}$  changes from 0 up to 10. We calculated polarization for  $q = 0; 0.05; 0.1; 0.5$ . For values  $\sqrt{\delta_0} > 10$  relatively good results can be obtained by extrapolation from  $p_l = 100 p_l(\sqrt{\delta_0} = 10)/\delta_0$  and for positional angles one must be taken  $\chi$  at boundary value  $\sqrt{\delta_0} = 10$  (see figures).

The peak value of the polarization occurs when  $\mathbf{M}$  is perpendicular to the line of sight. In this case  $\chi = 0$ , i.e. the electric field of the integral polarization oscillates in the plane ( $\mathbf{nM}$ ). For  $\delta_0 > 100$  and  $q = 0$  we have the asymptotic formula

$$p_l \cong \frac{6\%}{n\delta_0} \quad (19)$$

where  $n = 3, 1, 2$  corresponds to total dipole (14), diamagnetic envelope (15) and Parker's outflow (16), respectively. In figures these cases denoted as a), b) and c).

In the case  $\vartheta_m = 90^\circ$  the expressions (14), (15) and (16) for  $\delta \cos \Theta$  differ only in different coefficients before  $\delta_0$  ( $n = 3, 1, 2$ , correspondingly). For this reason, the peak polarization  $p_{l\max}$  in all cases is the same but due to the different factors corresponds to different values of  $\sqrt{\delta_0}$ . For the cases (14), (15) and (16),  $p_{l\max}$  occurs at  $\sqrt{\delta_0}$  to be equal to 1.385; 2.4 and 1.895, respectively. Of course,  $p_{l\max}$  depends on the true absorption degree  $q$ . The calculations show that  $p_{l\max}$  increases monotonically from 0.307% at  $q = 0$  up to 1.01% at  $q = 0.5$ .

The figures demonstrate that the position of  $p_{l\max}$  depends weakly on the angle between  $\mathbf{M}$  and line of sight  $\mathbf{n}$ . For this reason, one can give, the common for all  $\vartheta_m$  - angles, approximate formula for wavelength  $\lambda_{max}$  when the peak polarization occurs. For  $q = 0$  the values  $\sqrt{\delta_0}$ , mentioned above, give rise to the expression:

$$\lambda_{max} \approx \frac{2.68}{\sqrt{n B_0}} (\mu m), \quad (20)$$

where  $n = 3, 1, 2$  corresponds to the models (14), (15) and (16). Formula (20) allows us to estimate the magnetic field  $B_0$  on the outer surface of spherical envelope if the value  $\lambda_{max}$  is found from polarimetric observations. For  $q \neq 0$  one can obtain the analogous formula.

The procedure is the following: from b) - curve one can find the value  $(\sqrt{\delta_0})_{max}$ , divide it by  $\sqrt{0.8} = 0.894$  and take the number instead 2.86 in (20). For  $q = 0.5$  such procedure gives 2.07 instead of 2.68, i.e. the existence of absorption changes the estimation of  $B_0$  only slightly. Roughly, one can take  $\lambda_{max}(\mu m) \approx B_0^{-1/2}(G)$ .

Let us discuss now how to know from the polarimetric data whether the envelope is optically thin or optically thick. First of all, remember that the polarization degree of radiation, scattered in optically thin envelope, as a rule is sufficiently higher than that for optically thick envelope. But, the dilution effect from the nonpolarized radiation can decrease this difference. For example, the question arises from the analysis of AGN polarimetric data how the dilution effect from the neighboring stars is significant. It seems more informative to consider the spectral differences of polarization in these cases. The optical depth of the envelope, in principle, depends on wavelength. It can give the jump of positional angle at some  $\lambda$ . This means the transition from optically thin envelope to the optically thick one (see the monograph [1]). The calculations in [8,9,11] for optically thin envelopes are made only for pure dipole field (the case (a) in our figures). Therefore, we shall compare only upper figures with the curves in Fig.1.

The curves of the polarization degree  $p_l$  in both types of envelopes are qualitatively similar. First, the increasing of  $p_l \propto \lambda^4$  takes place, then the peak exists and finally polarization degree decreases. This decreasing depends on the explicit form of number density  $N_e(r)$ . For envelopes with permanent concentration ( $N_e = const$ ) we have  $p_l \propto \lambda^2$  at large values of  $\lambda$ . This dependence coincides with the corresponding asymptotic behavior in the case of optically thick envelope. But, most probably the number density of free electrons falls with the removal from the central source. If  $N_e(r)$  is proportional to  $r^{-2}$ , then in the case of optically thin envelope the polarization degree decreases as  $\propto 1/\sqrt{\lambda}$  whereas optically thick envelope gives  $p_l \propto 1/\lambda^2$ .

Thus, the form of the polarization spectra at large wavelengths allows to say whether the envelope is optically thin or thick. Unfortunately, the value of polarization at large wavelength can be very small (see (19)) and be undetectable from observations. Besides, the asymptotic region of large wavelengths depends on unknown magnetic field  $B_0$  on the outer surface of the envelope.

To estimate the magnetic field  $B_0$  for both types of envelopes we need to know the spectrum of polarization near the  $p_{lmax}$  value, i.e. we need to know  $\lambda_{max}$ . After that we can use the relation (20) in the case of optically thick envelope. Analogous expressions for optically thin envelopes are presented in [8,9]. For most probable distribution  $N_e \propto r^{-2}$  the spectrum of polarization of optically thin envelope has the peak at the following  $\lambda_{max}$ :

$$\lambda_{max} \approx \frac{4.65}{\sqrt{B_s \tau_{env}}} \approx \frac{4.65}{\sqrt{B_0 \tau_{env}}} \cdot \frac{R_s^{3/2}}{a^{3/2}}. \quad (21)$$

Here,  $B_s = M/R_s^3$  is the dipole magnetic field at the surface of central radiation source. The dipole law gives  $B_0 = B_s R_s^3/a^3$ . Because of  $R_s < a$  and  $\tau_{env} \leq 1$ , the estimation (21) gives rise to larger value for  $\lambda_{max}$ , than the estimation (20). It should be noted that for very large  $B_0$  the value  $\lambda_{max}$  can be in the X-ray range of the wavelengths. If the value  $B_0$  is assumed to be known then the estimations from asymptotic formulae can be made without knowledge of  $\lambda_{max}$ .

The spectra of the positional angles  $\chi$  for optically thin and thick envelopes are different. Generally speaking, this fact gives an additional opportunity to distinct these both cases. However, if the observed polarization corresponds to large wavelengths (when  $\delta_0 \gg 1$ ) then in both cases the angle  $\chi$  has practically permanent value and sign. In this case we can say nothing to resolve the dilemma. Really, the spectrum of  $\chi$  is useful for this aim, when it is known near  $\lambda_{max}$ , where the behavior of spectra for both cases is very different.

In the region of  $\delta_0 \ll 1$  the  $\chi$ -spectrum is practically useless as it seems that the signs of  $\chi$  are different in these cases. The sign of  $\chi$  depends on the dipole orientation which, as a rule, is unknown. If  $\mathbf{M}$  changes orientation to opposite one, then  $\chi$  changes its sign. However, if from some reasons we know the  $\mathbf{M}$  - orientation, then, in contrary, the observed sign of  $\chi$  demonstrate directly what type of envelope exists - optically thin or optically thick.

Table 3: The net polarization  $p_l$  of hot stars for various magnitudes of equatorial magnetic field.

Objects	$\tau_T$	$B_l = 100\text{G}$	$B_l = 10\text{G}$
$\zeta$ Puppis	0.2	$p_l = 0.4\%$	0.02%
$\varepsilon$ Ori	0.17	0.17%	0.01%
Deneb	0.03	0.01%	$\ll 0.01\%$
P Cyg	1	0.1%	0.3%
WR40	3.4	0.1%	0.3%

## 5 SOME ASTROPHYSICAL APPLICATIONS

### 5.1 Polarization of radiation from OB and WR stars: the estimation of a magnetic field

The hot stars are characterized by very strong,  $\sim \dot{M} \geq 10^{-5} M_\odot$ , outflow of a matter in form of the dense stellar wind (see [16-18]). The Thomson optical depth  $\tau$  of such wind can be both less ( $\zeta$  Puppis, Deneb) and greater (of the order) than unity (P Cyg, WR 40)(see [17]). The problem of the determination of surface magnetic field for these objects exists for a long time. In the paper [19] the positive answer is given for the question whether dipole magnetic field can exist at the surface of these stars.

The attempts to measure the magnetic fields of bright stars by the traditional circular polarization technique were unsuccessful [16,20]. Particulary, in the paper [20] the upper limit of the magnetic field component along the line of sight was obtained for the star 04I(n)f  $\zeta$  Puppis:  $B_{||} \leq 200\text{G}$ . The sufficient variability of the Stokes parameter  $V$  was not also found. One can expect that future Spectro-Polarimetric Interferometer (SPIN) will be useful.

Using our calculations (Fig.1 and 2) one can estimate the polarization in V-band for a number of stars from the list of objects of the project SPIN [17]. So, assuming that equatorial magnetic field  $B_e \approx 10^2\text{G}$  we obtain  $\delta_0 \approx 0.8\lambda_V^2 B_e \approx 24.2$ . If  $B_e \approx 10$  then we have  $\delta_0 \approx 2.42$ . The values of expected polarization degree are presented in Table 3 (for the inclination angle  $i = 90^\circ$ ). In estimations we have chosen the wind density distribution from the paper [21].

### 5.2 Polarization of radiation from the system Cyg X-1/HDE 226868

In 1975 Nolt et al. [22] have discovered the intrinsic linear polarization of the optical radiation of close binary system Cyg X-1/HDE 226868 with a compact component being a black hole with the mass  $\sim 10M_\odot$ . The polarization has variations with the amplitude  $\sim 0.2\%$ . The time behavior of polarization is rather complex. Besides the period of the binary system  $P = 5^{d.6}$ , the polarization varies with  $39^d$  and  $78^d$  characteristic times [22]. The possible mechanisms of the polarization of this system were discussed in [26].

If the polarized radiation arises in the accreting matter around the black hole the value of intrinsic polarization is to be some tens times higher than the observed value. It seems there exists very strong dilution by the unpolarized emission of supergiant HDE 226868. The luminosity of this star is estimated as  $L_0 \approx (1 \div 3) \times 10^{39} \text{ erg s}^{-1}$  whereas the X-ray luminosity of Cyg X-1 is about  $L_X \leq 8 \times 10^{37} \text{ erg s}^{-1}$  [23]. If optical radiation of the accretion disk arises as a result of the transformation of X-ray emission of the black hole then the value of intrinsic polarization have to be near the value  $p_l \leq 10\%$ . Optically thick accretion disk with most probable inclination  $i = 30^\circ$  can not produce such high polarization. For this reason if the polarization originates into accreting matter, then this polarization can arise only as a result of the scattering in optically thin coronae or in some sort of outflow from the accretion disk (wind). At the same time, it is not possible to exclude the mechanism of the production of small (at the level of some tens percents) intrinsic polarization from the star HDE 226868 in a magnetized stellar wind.

We consider both mechanisms and the corresponding consequences.

In the case of optically thin magnetized corona around the accretion disk the large,  $\sim p_l \sim 10\%$ , polarization can be produced if the central source is point-like or the coronae itself is very vast. For such model one can use the calculations of Dolginov et al. [1]. According to their calculations  $p_l \sim 10\%$  can be obtained at  $\delta_0 \tau_{env} \approx 10$  and when magnetic field is perpendicular to the line of sight. For  $i = 30^\circ$

it means that the magnetic field lies almost in the plane of the disk. If one supposes  $\tau_{env} \approx 0.1$  then the condition  $\delta_0 \approx 100$  (remember that  $\delta_0 \tau_{env} \approx 10$ ) gives rise to the estimation  $B_0 \approx 500 G$ . In a number of models the inner radius of a hot corona is determined as  $\sim 100 R_g$ , where  $R_g = 25M/c^2$  is the gravitational radius. In this case for dipole magnetic field follows the estimation  $B(3R_g) \sim 10^7 G$ .

Let us now consider the situation when the linear polarization is generated in the extended stellar wind of the optical component HDE 226868. The existence of such wind was confirmed by observation of modulated radio emission from Cyg X-1. The radio emission of the relativistic jet of the black hole has variable absorption in the plasma of the stellar wind. Modulation arises in the process of the orbital motion of the black hole [27].

Supposing that in stellar wind  $N_e \sim r^{-2}$  and  $\dot{M} \approx 2 \times 10^{-6} M_\odot \text{ year}^{-1}$ ,  $R_s = 10R_\odot$  and  $V_\infty \approx 1850 \text{ km s}^{-1}$  [27], one can estimate the Thomson optical depth of the wind as  $\tau_T \approx 0.1$ . According to Fig.1 the polarization  $p_l \approx 0.2\%$  corresponds to the angle between magnetic dipole  $\mathbf{M}$  and line of sight being  $\sim 65^\circ$  and the parameter  $\sqrt{\delta_S \tau_{env}} \approx 3$ . It gives the estimation  $B_s \approx 350 G$ . Such value of extremal magnetic field for the OV supergiant seems to be rather large. It is interesting that in this case the dipole axis lies in the orbital plane and one has not any problems to explain the variability of the polarization.

### 5.3 Intrinsic polarization of SS 433

The famous galactic X-ray binary system SS 433 is the microquasar with two relativistic ( $V \approx 0.26c$ ) strongly collimated ( $\vartheta \approx 1^\circ$ ) jets. The system is characterized by 3 periodic motions: the orbital motion with the period  $P_o = 13^d.082$ , the precession with  $P_p = 162^d.5$  and nutation with  $P_n = 6^d.28$  [23,28]. Recent spectral observations [20] confirm the existence of spectral absorption lines of the A7Ib supergiant. The mass ratio of the relativistic component and an optical star is about  $q = M_X/M_V = 0.57 \pm 0.11$ . The masses of every component are estimated as  $M_V = (19 \pm 7)M_\odot$ ,  $M_X = (11 \pm 5)M_\odot$  [28]. The kinematics of relativistic jets allows to estimate the inclination angle of the orbital plane  $i = 78^\circ.82 \pm 0^\circ.11$ . The precession angle  $\theta$  of a disk is equal to  $\theta = 19^\circ.80 \pm 0^\circ.18$ .

The variable, i.e. intrinsic, polarization of SS 433 first was observed by McLean and Tapia [30], and later, in B, V, R, I bands, by the observers in KrAO [31]. In 1993 the polarimetric observations of SS433 were obtained in UV range by high speed photometer-polarimeter (HSP) from the cosmic Hubble telescope [32]. The polarization degree in UV range is rather high  $p_l = (13.4 \pm 4)\%$  and it demonstrates the time variability. Such a high degree of polarization can not originate in an accretion disk. Most probably it is a result of the scattering of radiation by free electrons in a plasma outflow (for example, in a hot corona or wind). An example of such plasma can be, also, optically thin advective accretion flux around the black hole [33].

We calculated the expected polarization degree of the radiation scattered in a spherical stellar wind with the Parker's type magnetic field

$$B_r = B_p(R_A/r)^2 \cos \theta; \quad B_\varphi = B_T \frac{R_A}{r} \sin \theta; \quad B_\theta = 0 \quad (22)$$

where  $B_p$  is the magnetic field at magnetosphere's pole,  $B_T$  is the value of toroidal component,  $R_A$  is the radius of the magnetosphere. There was used the technique described in the papers [1,8-10].

The results are presented in Fig.6. They are compared with the observational data of Dolan et al. [32]. We assumed that the Thomson optical depth of the coronae is near unity, i.e.  $\tau_T \leq 1$ .

The results of UV polarimetric observations corresponds rather well to the theoretical curve if one assumed  $B_p = 1 G$  and  $B_T = 600 G$ . The disagreement between observational polarization and the theory in optical range can be explained by the existence of the dilution from intrinsic non-polarized radiation of the accretion disk. However, the Thomson polarization of radiation outgoing from plane-parallel disk at  $i \approx 80^\circ$  is rather high ( $p_l \approx 5\%$ , [13]), the strong ( $B_T \approx 600 G$ ) toroidal magnetic field depolarizes fully the scattered radiation because of the depolarization parameter  $\delta_0$  is very large ( $\delta_0 \geq 500(\lambda/1\mu\text{m})^2$ , see (21)).

It is interesting that our estimation of the magnetic field near the magnetosphere allows us to obtain the additional information about the parameters of the accretion to the black hole itself.

The modern theory of rotating black holes determines the magnetosphere as a region from which the relativistic jets outflow occurs and, simultaneously, arises the hot corona [4,34]. According to [34], the radius  $R_A \approx 5 \times 10^3 R_g$  in the case of pure thermal coronae and  $R_A \approx 300 R_g$  for the, so called, hybrid coronae. As a result one can estimate the value of magnetic field in the vicinity of black hole, near the last stable orbit  $3R_g$  ( $R_g$  is the gravitational radius). If one assumed that the estimation (21) for

Parker's type of magnetic field is valid up to  $3R_g$ , then we obtain the estimation of the magnetic field of the black hole in SS 433 as  $B_{max} \approx 10^4 \div 10^6 G$ , depending on the type of coronae. This value is in a good agreement with that in the model of Blandford and Znajek [4].

It should be noted that if one takes  $R_A \approx 10^{10} cm$  (as in [34]) then the value of magnetic moment  $\mu$  of the compact component in SS 433 can be estimated as  $\mu \approx 10^{34} G cm^3$ . This value is near the value of  $\mu$  for another microquasar GRS1915+05 obtained by Robertson and Leiter [2] from very different consideration.

Finally, if, according to [33], one considers that the magnetic force lines strongly follow the motion of the plasma in the accretion disk, then we can estimate the known viscosity factor  $\alpha$  of the Sunyaev-Shakura theory [35]. According to

$$\frac{B_r}{B_\varphi} = \frac{U_r}{U_\varphi} \approx \alpha \quad (23)$$

where  $U_r$  and  $U_\varphi$  are the radial and Keplerian velocities in accretion disk, correspondingly. Our estimation of  $B_r$  and  $B_\varphi$  gives rise to  $\alpha \approx 2 \times 10^{-3}$  what is practically coincides with the theoretical estimation in [36].

#### 5.4 Polarization of radiation of supernovae

Recently a lot of observational data has been obtained giving an evidence that the radiation from supernovae has a sufficient polarization (see the review [37]). In particular, the spectropolarimetric observations of young supernovae, obtained at Kek-telescope, demonstrate that the intrinsic polarization exists for all the types of supernovae [38]. These observations, for example, show that the supernovae 1997dt (Ia), 1998T and 1997dq (both of the type Ib), 1997ef (Ib/c - peculiar), 1997eq (IIn), 1997ds (II-p) have intrinsic polarization. It was shown [39] that the supernovae of types II and Ib/c are polarized at the level  $p_l \approx 1\%$ . Some of them have higher polarization. It is interesting (see [39]) that the lesser is the hydrogen envelope and the deeper layers are seen the larger is the value of polarization. Such dependence was analyzed by Hofflich et al. [40]. It proved to be the case that the observed polarization is higher for SN II as compared with SN Ic.

It is natural, that many authors explain the observed polarization as due to the scattering of radiation in asymmetric envelope of the expulsed matter (see, for example, [37]).

There exists another physical mechanism that can be responsible for the noticeable net polarization of SN radiation without asymmetric distribution of the exploded matter.

Such mechanism is the considered above integral effect of the Faraday rotation of the polarization plane of the radiation scattered in the spherically symmetric envelope of exploded matter (blow shock) with a magnetic field. Namely this effect produces the intrinsic polarization. The measured net polarization allows to estimate the magnetic field strength in the region of propagating blow shock.

Now let consider some examples. The supernova SN IIp 1999em was observed at epochs of 7, 40, 49, 159 and 163 days after the explosion and its radiation was to be polarized at these epochs (Leonard et al., 2001). The detected net polarization was  $p_l \sim (0.2 \div 0.5)\%$ . This magnitude is quite well corresponding to the results of our calculations presented at Fig.2, the polarization maximum corresponding to the Faraday depolarization parameter  $\delta_0 \sim 4$ . For the visual magnitude (V band -  $\lambda_{eff} = 0.55\mu m$ ) this value of the depolarization parameter allows to determine the magnetic field strength as  $B \approx 16.5 G$ .

Another example is SN Ia. The typical value of the intrinsic polarization of such kind supernovae is to be  $p_l \approx 0.7\%$  (Kasen et al., 2003). This value of polarization is better corresponding to our results presented at Fig.1, i.e. to the case of scattering into the magnetized optically thin envelope. In this case the real depolarization parameter is  $(\delta_S \tau_T)^{1/2}$ , where  $\tau_T \ll 1$  is the optical thickness of an envelope with respect to the electron scattering. The polarization magnitude  $p_l \sim 1\%$  corresponds to the depolarization parameter value of  $(\delta_S \tau_T) \sim 1$ . In this case the magnetic field strength is  $B_s \sim 4/\tau_T G$ . For  $\tau_T \sim 0.1$  the magnetic field strength in the shock region can reach the strength  $\sim 40 G$  and even  $\sim 100 G$ .

The calculation of non-sphericity of an envelope is not principal problem. Some cases of generation of polarized radiation in a magnetized non-spherical envelope was considered in [1,14].

## 6 CONCLUSIONS AND OUTLOOK

We represented the results of calculations of the integral polarization of radiation emerging from the optically thick spherically symmetric envelope with the dipole magnetic field of a central radiation source (a neutron star; extended supernova envelopes produced by the supernova explosion at the initial stage of expansion; accretion flows around quasars and active galaxy nuclei). We considered also the cases of diamagnetic (perfectly conducting) plasma envelope when the normal component of magnetic field does not penetrate inside a disk and radially evaporated envelope. The comparison of the results of polarization between the various types of envelopes have been made.

The results of our theoretical calculations can be used for the analysis of polarimetric observations of hot stars, including WR stars, X-ray binaries (Cyg X-1/HDE 226868, SS 433), supernovae and etc. We plan to use the results of our calculations to an analysis of polarimetric data of quasars and AGNs (see, for example, [44]).

This work is partially supported by the RFBR grant 03-02-17223, the Program of the Prezidium of RAN "Nonstationary Phenomena in Astronomy", the Program of the Department of Physical Sciences of RAN "The Extended Structures..." and by the Program of Astronomy of Russian Science and Education Ministry.

## References

- [1] A. Z. Dolginov, Yu. N. Gnedin, N. A. Silant'ev, *Propagation and polarization of radiation in cosmic media* (Gordon and Breach Publs., Amsterdam, 1995)
- [2] S. L. Robertson and D. J. Leiter, *Astrophys.J.*, **596**, October 20 (2003).
- [3] Yu. N. Gnedin, N. V. Borisov, T. M. Natsvlishvili, M. Yu. Piotrovich, *astro-ph/0304158*.
- [4] R. D. Blandford and R. L. Znajek, *MNRAS*, **179**, 433 (1977).
- [5] L. -X. Li, *astro-ph/0202361*.
- [6] F. M. Rieger and K. Manheim, *astro-ph/0011012*.
- [7] A. Tomimatsu and M. Takakashi, *Astrophys.J.*, **552**, 710 (2001).
- [8] Yu. N. Gnedin and N. A. Silant'ev, *Pisma AZh*, **6**, 344 (1980).
- [9] Yu. N. Gnedin and N. A. Silant'ev, *Asrophys.Sp.Sci.*, **102**, 375 (1984).
- [10] N. A. Silant'ev, Yu. N. Gnedin, and T. Sh. Krymski, *Astron.Astrophys.*, **357**, 1151 (2000).
- [11] M. A. Pogodin, *Pisma AZh*, **18**, 442 (1992).
- [12] E. Agol, O. Blaes, and C. Ionescu-Zanetti, *MNRAS*, **293**, 1 (1998).
- [13] P. S. Shternin, Yu. N. Gnedin and N. A. Silant'ev, *Astrofizika*, **46**, 433 (2003).
- [14] N. A. Silant'ev, *Astron.Astrophysics*, **383**, 326 (2002).
- [15] D. Lai, *Astrophys.J.*, **524**, 1030 (1999).
- [16] J. Babel and T. Montmerle, *Astrophys.J.Lett.*, **485**, L29 (1997).
- [17] O. Chesneau, S. Wolf, and A. Domiciano de Souza, *astro-ph/0307407*.
- [18] M. E. Contreras, G. Montes and F. P. Wilkin, *astro-ph/0310393*.
- [19] A. B. Underhill and R. P. Fahey, *Astrophys.J.*, **280**, 712 (1984).
- [20] O. Chesneau and A. F. J. Moffat, *PASP*, **114**, 612 (2002).
- [21] J.P. Cassinelli, N.M. Hoffman, *MNRAS*, **173**, 789 (1975).
- [22] I.G. Nolt, J.C. Kemp, R.J. Rudy et al., *Ap.J.L.*, **199**, L27 (1975).

- [23] A. M. Cherepashchuk, *Uspehi Fiz. Nauk*, **171**, 864 (2001).
- [24] N. G. Bochkarev, E. A. Karitskaya, R. A. Sunyaev, N. I. Shakura, *Astron.Zh.*, **55**, 185 (1979).
- [25] E. A. Karitskaya, *Astron.Zh.*, **58**, 146 (1981).
- [26] Yu. N. Gnedin, N. V. Borisov, T. M. Natsvlishvili, M. Yu. Piotrovich, N. A. Silant'ev, *astro-ph/0304158*, *Astrophys.Sp.Sci.*, in press (2004).
- [27] C. Brocksopp, R. P. Fender and G. G. Pooley, *astro-ph/0206460*, *MNRAS* in press (2003).
- [28] A. M. Cherepashchuk, R. A. Sunyaev, E. V. Seifina, I. E. Panchenko, S. V. Molkov, K. A. Postnov, *astro-ph/0309140* (2003).
- [29] D. R. Gies, W. Huang and M. V. McSwain, *Astrophys.J.*, **579**, 67 (2002).
- [30] I. S. McLean and S. Tapia, *Nature*, **287**, 704 (1980).
- [31] Y. S. Efimov, V. Pirola and N. M. Shakhovskoy, *Astron.Astrophys.*, **138**, 62 (1984).
- [32] J. F. Dolan, P. T. Boyd, S. N. Fabrika, *et al.* *Astron.Astrophys.*, **327**, 648 (1997).
- [33] L. -X. Li, *astro-ph/0112503* (2002).
- [34] T. J. Maccarone and P. S. Coppi, *astro-ph/0204235* (2002).
- [35] N. I. Shakura and R. A. Sunayev, *Astron.Astrophys.*, **24**, 377 (1973).
- [36] A. R. King, J. E. Pringle, R. G. West, M. Livio, *astro-ph/0311035* (2003).
- [37] L. Wang, D. Baade, P. Höflich, J. C. Wheeler, *The Messenger*, **109**, 47 (2002).
- [38] D. C. Leonard, A. V. Filippenko, A. J. Barth, T. Matheson, *Astrophys.J.*, **536**, 239 (2000).
- [39] J. C. Wheeler, P. Höflich, L. Wang, I. Yi, *astro-ph/9912080* (1999).
- [40] P. Höflich, J. C. Wheeler, and L. Wang, *Astrophys.J.*, **521**, 179 (1999).
- [41] D. C. Leonard, A. V. Filippenko, and M. S. Brotherton, *Astrophys.J.*, **553**, 861 (2001).
- [42] D. Kasen, P. Nugent, L. Wang, *et al.* *astro-ph/0301312* (2003).
- [43] P. G. Martin, I. B. Thompson, J. Naza, J. R. P. Angel, *Astrophys.J.*, **265**, March 15 (1983).
- [44] Yu. N. Gnedin and N. A. Silant'ev, *Pisma AZh*, **28**, 490 (2002).

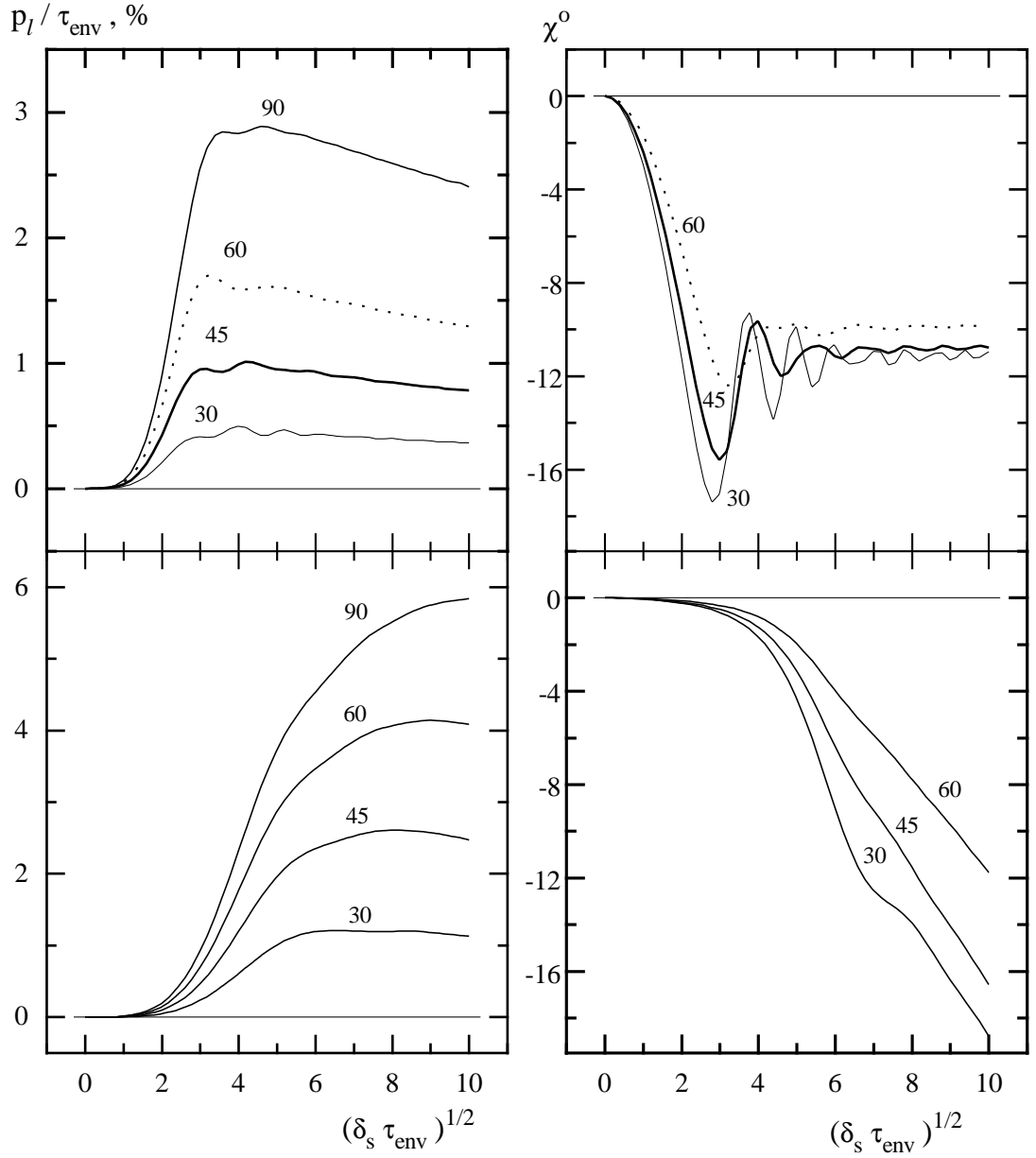


Figure 1: The polarization degree and the positional angle of the integral radiation of optically thin spherical envelope in the magnetic dipole field. The upper panels corresponds to the case  $N_e \sim r^{-2}$  and the low ones to the envelope with constant electron number density  $N_e = \text{const}$  with  $\eta = 5$ . The numbers near the curves denote the angle (in degrees) between the magnetic dipole  $\mathbf{M}$  and line of sight  $\mathbf{n}$ .

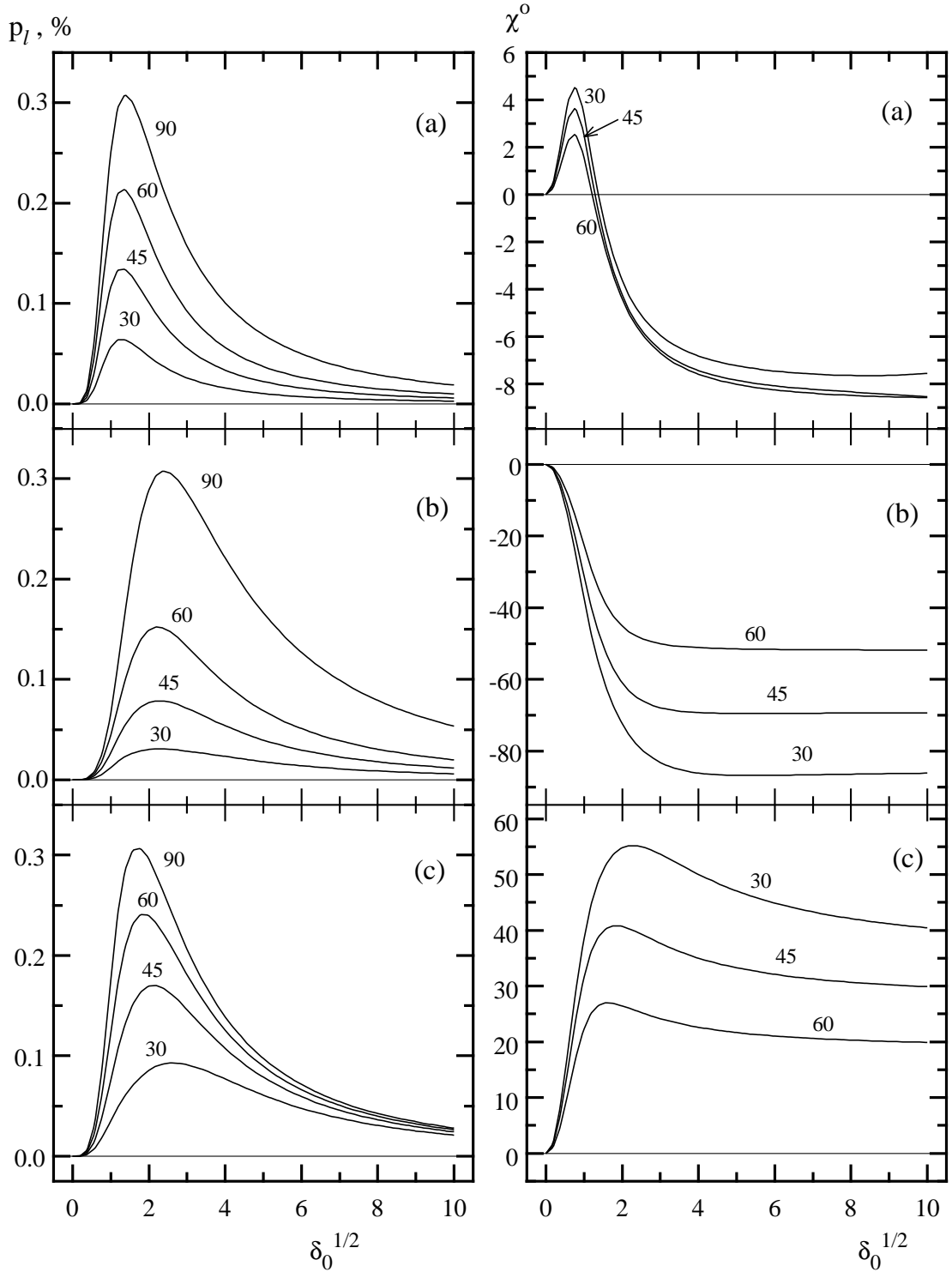


Figure 2: The polarization degree and the positional angle of the integral radiation of the optically thick magnetized for the conservative atmosphere ( $q = 0$ ). The numbers denote the angle  $\vartheta_m$  (in degrees) between the magnetic dipole  $\mathbf{M}$  and the line of sight  $\mathbf{n}$ . The cases a), b) and c) correspond to the total dipole field, diamagnetic atmosphere ( $B_r = 0$ ) and Parker's outflow field ( $B_r \neq 0$ ), correspondingly.

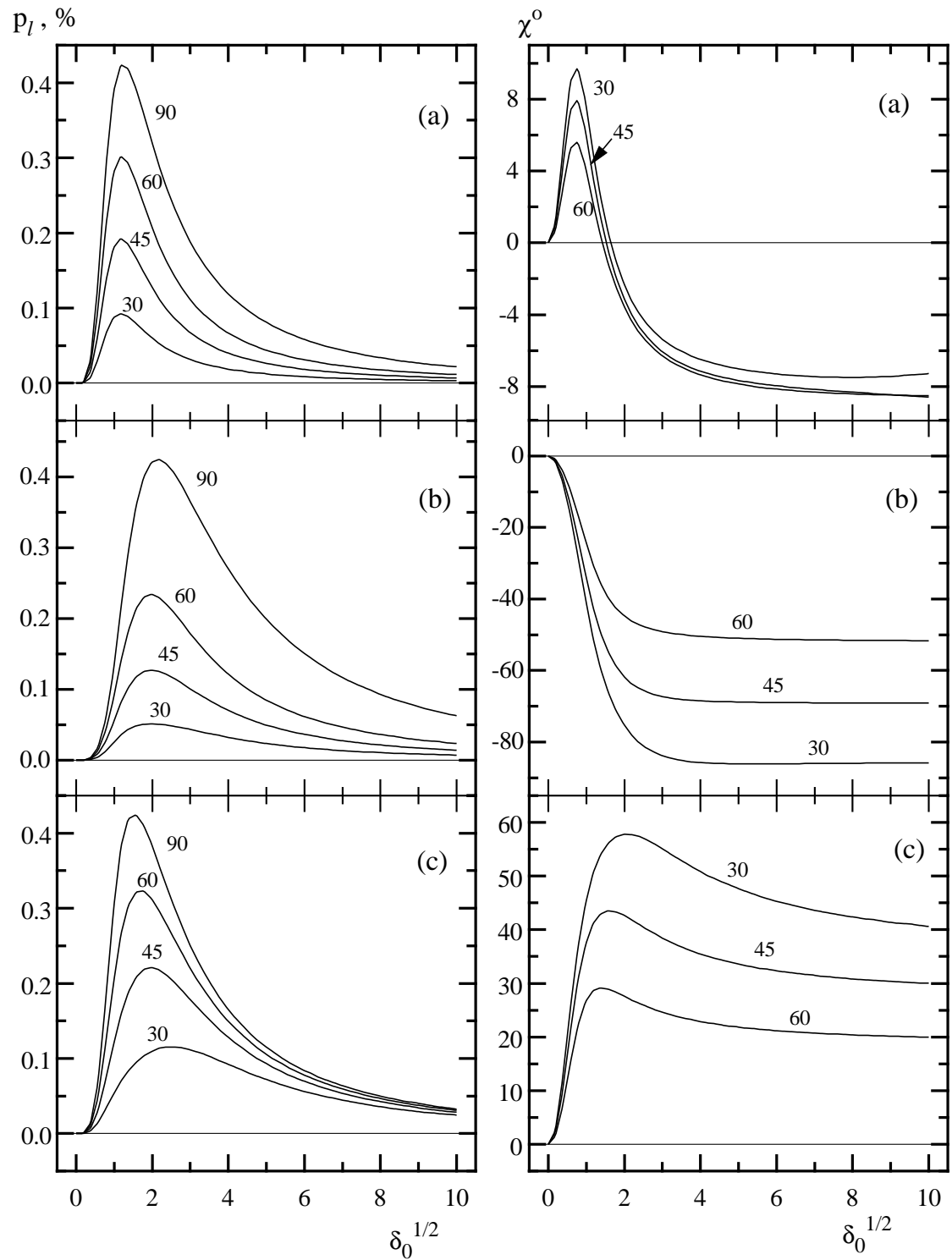


Figure 3: The same as in Fig.2, but for  $q = 0.05$ .

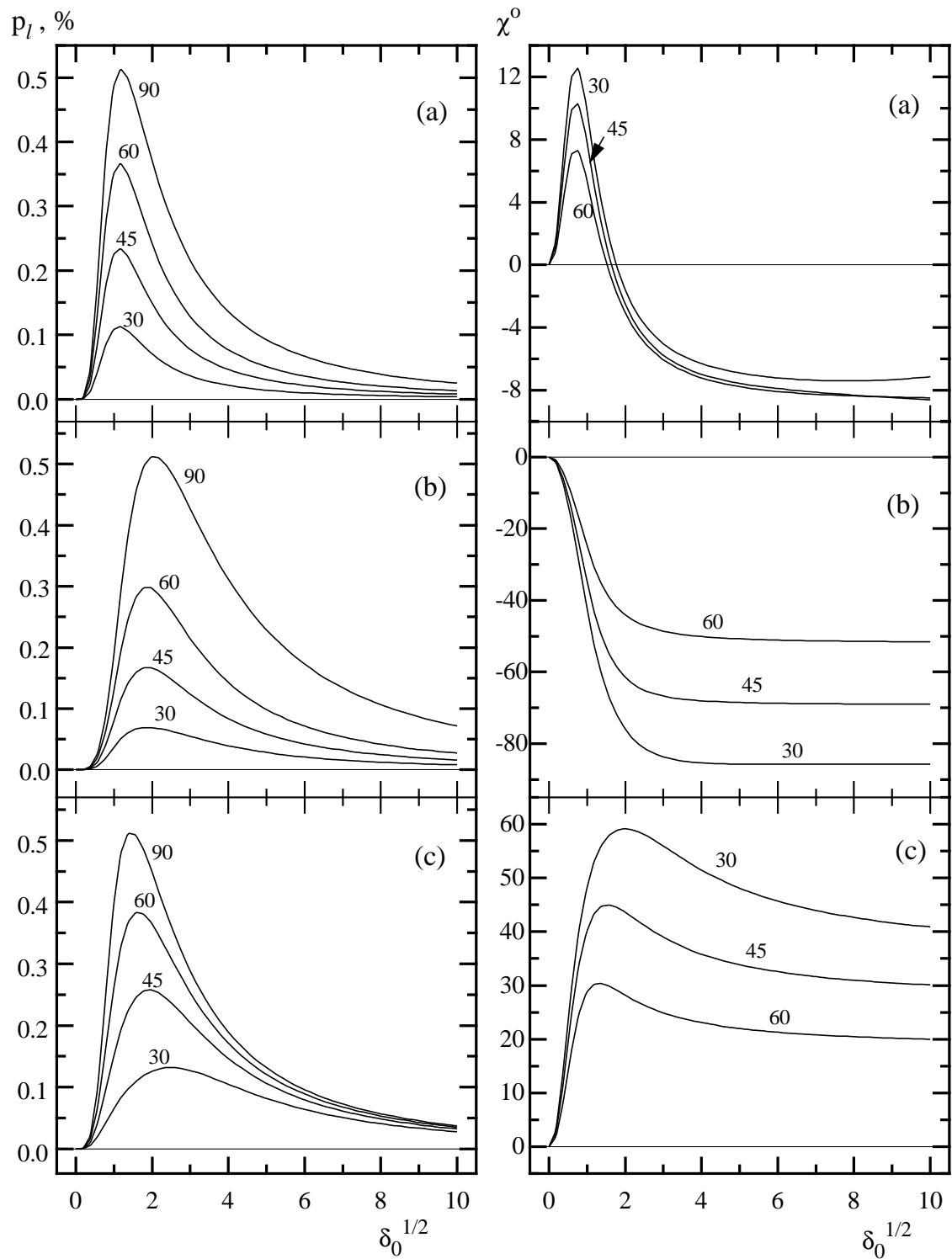


Figure 4: The same as in Fig.2, but for  $q = 0.1$ .

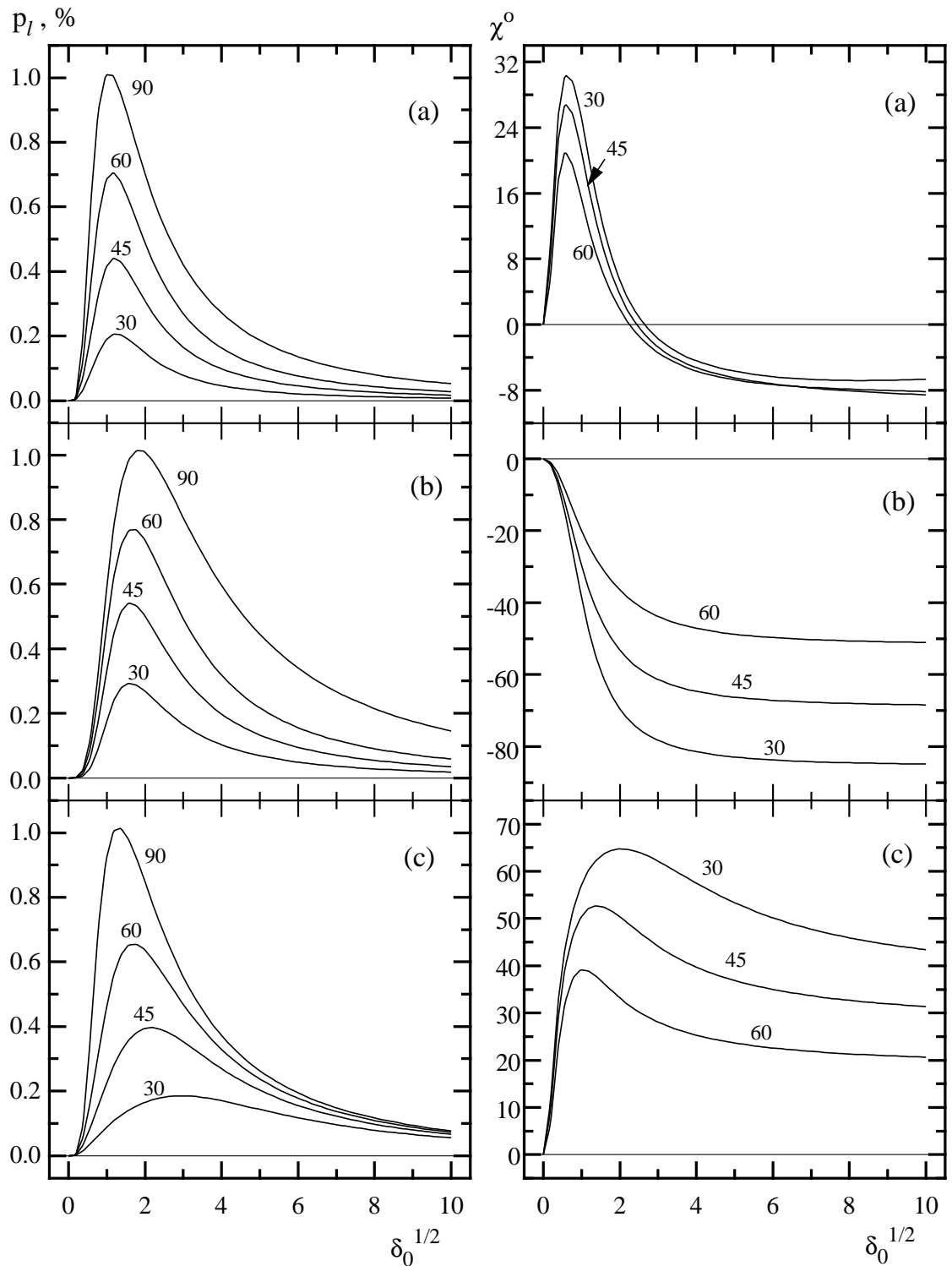


Figure 5: The same as in Fig.2, but for  $q = 0.5$ .

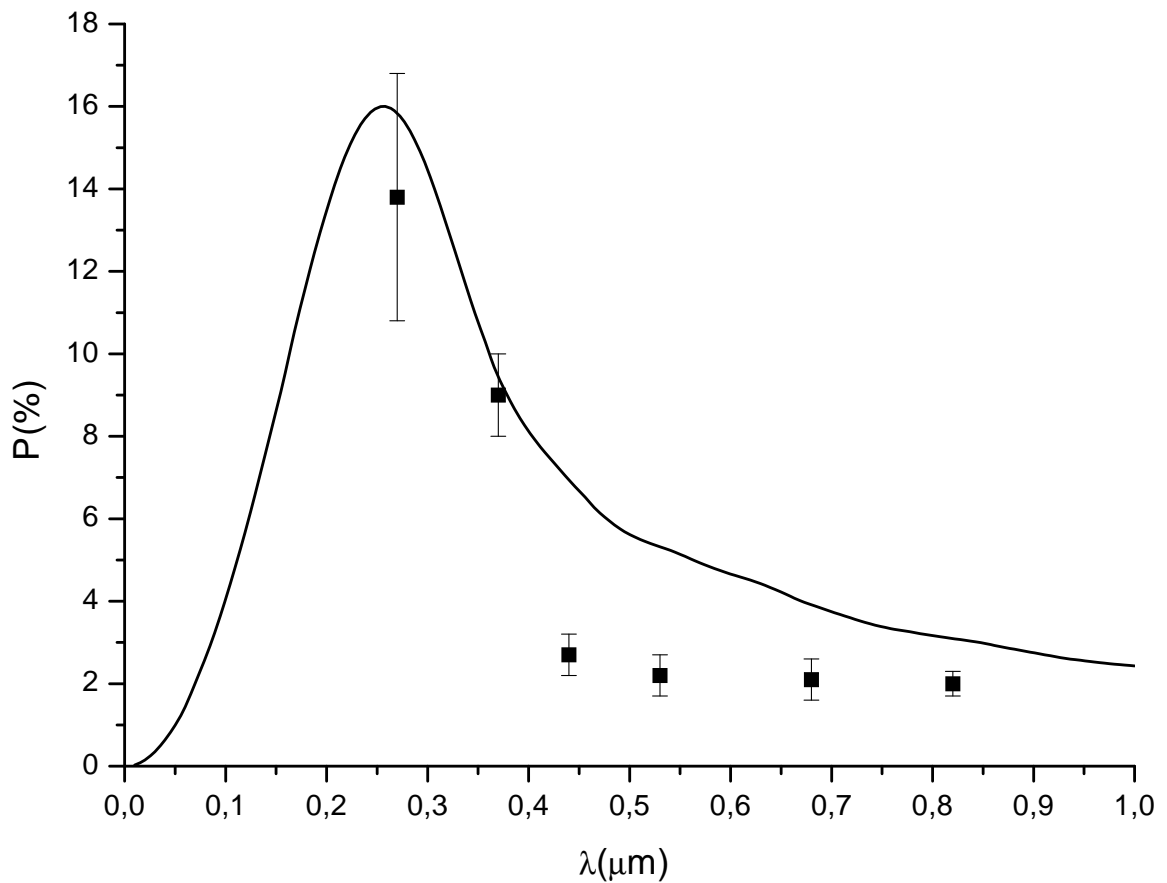


Figure 6: The spectrum of integral linear polarization of X-ray binary system SS433: comparison of the observational with the results of theoretical model (solid curve) at  $\tau_T = 1.0$ ,  $B_{Pol} = 1G$ ,  $B_{Tor} = 600G$ .